UNCLASSIFIED

AD <u>418708</u>

DEFENSE DOCUMENTATION CENTER

FOR

SCIENTIFIC AND TECHNICAL INFORMATION

CAMERON STATION ALEXANDRIA VIRGINIA

UNCLASSIFIED

Division of Engineering
BROWN UNIVERSITY
PROVIDENCE, R. I.

AFCRL-63-318

ON THE SCATTERING OF ELECTROMAGNETIC

WAVES BY A DIELECTRIC CYLINDER

BY

WILLIAM STREIFER and RALPH D. KODIS

ON THE SCATTERING OF ELECTROMAGNETIC WAVES

BY A DIELECTRIC CYLINDER

by

William Streifer and Ralph D. Kodis

Brown University

Providence, Rhode Island

ABSTRACT

The scattering of E-polarized cylindrical electro-magnetic waves by an infinitely long dielectric cylinder is investigated. For small incident wavelength the slowly converging series solution is converted to a sum of integrals. An expansion is performed so that the integrals may be divided into two classes depending on the relative locations of source and observation points. Those in the first class have points of stationary phase and an asymptotic evaluation gives contributions which are identified as those of geometric optics. The remaining integrals are evaluated as residue sums. A plot of normalized back-scattering cross section vs. normalized radius for $n = .4$ is given.

Introduction:

The scattering of electromagnetic waves by an infinite dielectric cylinder of large radius has been treated by Beckmann and Franz [1] , [2] among others. They employ the Watson transformation to convert the slowly convergent series solution into a sum of integrals, some of which are evaluated by the method of stationary phase and yield geometric optics terms. The remainder are transformed to residue sums and interpreted as diffraction effects. The pole locations they use in evaluating these residues are only qualitatively determined.

In the following the authors employ the Poisson sum formula as suggested by Wu [3] to obtain integrals similar to those found by Beckmann and Franz. However, the present work is an extension of theirs in three respects: (1), more precise pole locations are used in the residue computation; (2), the refractive index of the cylinder is taken to be less than one; and (3), numerical results are included.

Formulation:

If an electromagnetic wave emanates from an infinite line source with its electric vector parallel to the axis of an infinite dielectric cylinder, the governing equation in the coordinate system illustrated in figure 1 is

$$\left[\nabla_{r\theta}^2 + k^2(r) \right] G(\bar{r},\bar{r}') = -\delta(\bar{r}-\bar{r}'),$$

(1)

where

$$k(r) = \begin{cases} k_1 & r < a \\ k_2 & r > a, \end{cases} \qquad k_1, k_2 \text{ real.}$$

The function $G(\vec{r}, \vec{r}')$, together with its derivative $\partial_r G(\vec{r}, \vec{r}')$, is continuous at the cylinder surface $r = |\vec{r}| = a$ and satisfies the radiation condition

$$\lim_{r \to \infty} \left[r^{1/2} (\partial_r - ik_2) G \right] = 0.$$

The solution of (1) in $r \geq a$, found by separation of variables, is

$$G(\vec{r}, \vec{r}') = \sum_{n=-\infty}^{\infty} \frac{i}{8} \left[H_n^{(1)}(k_2 r') H_n^{(2)}(k_2 r) + H_n^{(1)}(k_2 r') H_n^{(1)}(k_2 r) \frac{H_n^{(2)'}(x)}{H_n^{(1)'}(x)} R(n) \right] e^{in\theta}, \qquad (2a)$$

where

$$R(n) = - \frac{x \dfrac{H_n^{(2)'}(x)}{H_n^{(2)}(x)} - y \dfrac{J_n'(y)}{J_n(y)}}{x \dfrac{H_n^{(1)'}(x)}{H_n^{(1)}(x)} - y \dfrac{J_n'(y)}{J_n(y)}}, \qquad (2b)$$

and $\quad x = k_2 a, \quad y = k_1 a$

The line source may be at either the primed or unprimed point, provided $r' > r$

For large cylinders, i.e. $x, y \gg 1$, the series (2a) converges very slowly, and it is convenient to employ the Poisson sum formula [3] to obtain

$$G(\vec{r}, \vec{r}') = \sum_{m=-\infty}^{\infty} \frac{i}{8} \int_{-\infty}^{\infty} \left[H_\nu^{(1)}(k_2 r') H_\nu^{(2)}(k_2 r) + H_\nu^{(1)}(k_2 r') H_\nu^{(1)}(k_2 r) \frac{H_\nu^{(2)'}(x)}{H_\nu^{(1)'}(x)} R(\nu) \right] e^{i\nu\theta} e^{2\pi i m \nu} d\nu.$$

$$(3)$$

When Debye's asymptotic forms for the Hankel and Bessel functions [4] are substituted in (3) it is evident that for $0 \leq \theta \leq \pi$ every integral with $m \geq 0$ has many stationary phase points. These contributions may be separated by expanding $R(\nu)$ (See Appendix A):

$$R(\nu) = R_1(\nu) + (1+R_1)(1+R_2) \sum_{p=1}^{\infty} R_2^{p-1} \left[\frac{H_\nu^{(1)}(y)}{H_\nu^{(2)}(y)} \right]^p , \qquad (4)$$

where

$$R_1(\nu) = -\frac{1}{L(\nu)} \left\{ x \frac{H_\nu^{(2)'}(x)}{H_\nu^{(2)}(x)} - y \frac{H_\nu^{(2)'}(y)}{H_\nu^{(2)}(y)} \right\} ,$$

$$R_2(\nu) = -\frac{1}{L(\nu)} \left\{ x \frac{H_\nu^{(1)'}(x)}{H_\nu^{(1)}(x)} - y \frac{H_\nu^{(1)'}(y)}{H_\nu^{(1)}(y)} \right\} ,$$

and

$$L(\nu) = x \frac{H_\nu^{(1)'}(x)}{H_\nu^{(1)}(x)} - y \frac{H_\nu^{(2)'}(y)}{H_\nu^{(2)}(y)}$$

Substituting (4) in (3), interchanging summation and integration, and carrying out various algebraic manipulations, we obtain:

$$G(\vec{r},\vec{r}') =$$

$$= \sum_{m=-\infty}^{-1} \frac{i}{8} \int_{-\infty}^{\infty} \left[H_\nu^{(1)}(k_2 r') H_\nu^{(2)}(k_2 r) + H_\nu^{(1)}(k_2 r') H_\nu^{(1)}(k_2 r) \frac{H_\nu^{(2)}(x)}{H_\nu^{(1)}(x)} R(\nu) \right] e^{i\nu\theta} e^{2\pi i m \nu} d\nu +$$

$$\qquad (5a)$$

$$+ \sum_{m=1}^{\infty} \frac{i}{8} \int_{-\infty}^{\infty} \left[H_\nu^{(1)}(k_2 r') H_\nu^{(2)}(k_2 r) + H_\nu^{(1)}(k_2 r') H_\nu^{(1)}(k_2 r) \frac{H_\nu^{(2)}(x)}{H_\nu^{(1)}(x)} R(-\nu) \right] e^{i\nu\theta} e^{2\pi i m \nu} d\nu +$$

$$\qquad (5b)$$

$$+ \sum_{p=1}^{\infty} \sum_{m=1}^{p-1} \frac{i}{8} \int_{-\infty}^{\infty} H_\nu^{(1)}(k_2 r') H_\nu^{(1)}(k_2 r) \frac{H_\nu^{(2)}(x)}{H_\nu^{(1)}(x)} (1+R_1)(1+R_2) R_2^{p-1} \left[\frac{H_\nu^{(1)}(y)}{H_\nu^{(2)}(y)} \right]^p e^{i\nu\theta} e^{2\pi i m \nu} d\nu +$$

$$\qquad (5c)$$

$$+ \frac{i}{8} \int_{-\infty}^{\infty} \left[H_\nu^{(1)}(k_2 r')H_\nu^{(2)}(k_2 r) + H_\nu^{(1)}(k_2 r')H_\nu^{(1)}(k_2 r)\frac{H_\nu^{(2)}(x)}{H_\nu^{(1)}(x)} R_1(\nu) \right] e^{i\nu\theta}\, d\nu \ +$$

(5d)

$$+ \sum_{p=1}^{\infty} \frac{i}{8} \int_{-\infty}^{\infty} H_\nu^{(1)}(k_2 r')H_\nu^{(1)}(k_2 r)\frac{H_\nu^{(2)}(x)}{H_\nu^{(1)}(x)} (1+R_1)(1+R_2) R_2^{\nu-1} \left[\frac{H_\nu^{(1)}(y)}{H_\nu^{(2)}(y)} \right]^p e^{i\nu\theta}\, d\nu \ +$$

(5e)

$$- \frac{i}{\pi^2} \int_{-\infty}^{\infty} \frac{H_\nu^{(1)}(k_2 r')\, H_\nu^{(1)}(k_2 r)}{\left[H_\nu^{(1)}(x)\right]^2 H_{-\nu}^{(2)}(y)\, J_{-\nu}(y)} \frac{e^{i\nu\theta}}{L(\nu)\left\{ x\,\dfrac{H_\nu^{(1)'}(x)}{H_\nu^{(1)}(x)} - y\,\dfrac{J_{-\nu}'(y)}{J_{-\nu}(y)} \right\}}\, d\nu$$

(5f)

Each of the integrals (5a) - (5f) which has a stationary phase point yields a characteristic ray of geometric optics. Some of these rays can reach only a restricted region which depends upon the relative dielectric constant of the cylinder and the relative position of source and observation points. With the index of refraction $N = y/x < 1$ and the observation point at $r < r'$, three regions can be distinguished (see figure 1).

Region 1 - Forward Scattering

In this, the "shadow" region, it is convenient to rewrite $G(\bar{r},\bar{r}')$ in the form:

$$G(\bar{r},\bar{r}') =$$
$$= \sum_{m=-\infty}^{-1} \frac{i}{8} \int_{-\infty}^{\infty} \left[H_\nu^{(1)}(k_2 r')H_\nu^{(2)}(k_2 r) + H_\nu^{(1)}(k_2 r')H_\nu^{(1)}(k_2 r)\frac{H_\nu^{(2)}(x)}{H_\nu^{(1)}(x)} R(\nu) \right] e^{i\nu\theta} e^{2\pi i m\nu}\, d\nu \ +$$

(6a)

$$+ \sum_{m=0}^{\infty} \frac{i}{8} \int_{-\infty}^{\infty} \left[H_\nu^{(1)}(k_2 r')H_\nu^{(2)}(k_2 r) + H_\nu^{(1)}(k_2 r')H_\nu^{(1)}(k_2 r)\frac{H_\nu^{(2)}(x)}{H_\nu^{(1)}(x)} R(-\nu) \right] e^{i\nu\theta} e^{2\pi i m\nu}\, d\nu \ +$$

(6b)

$$+\sum_{p=1}^{p-1}\sum_{m=0}^{\infty}\frac{i}{8}\int_{-\infty}^{\infty}H_{\nu}^{(1)}(k_2 r')H_{\nu}^{(1)}(k_2 r)\frac{H_{\nu}^{(2)}(x)}{H_{\nu}^{(1)}(x)}(1+R_1)(1+R_2)R_2^{p-1}\left[\frac{H_{\nu}^{(1)}(y)}{H_{\nu}^{(2)}(y)}\right]^p e^{i\nu\theta}e^{2\pi i m\nu}d\nu,$$

(6c)

where (5c) and (5c) as well as (5d), (5f), and (5b) have been combined.

The denominator of (6c) contains the factor $H_{\nu}^{(1)}(y)H_{\nu}^{(2)}(y)$ which increases exponentially when $\nu > y$. The principle contribution of those integrals therefore occurs in the range ($-y,y$). Substitution of the Debye asymptotic forms in this interval yields

$$I_{pm} \sim (4\pi)^{-1}exp\left[i\pi(p-1)/2\right]\int_{-A}^{A}\frac{(1+R_1)(1+R_2)(-R_2)^{p-1}}{\{[(k_2 r')^2-\nu^2][(k_2 r)^2-\nu^2]\}^{1/4}}\left[1+O(\bar{y}^1)\right]d\nu,$$

(7a)

where

$$0 < y - A = O(y),$$

and

$$R_1 \sim -R_2 \sim \frac{(x^2-\nu^2)^{1/2}-(y^2-\nu^2)^{1/2}}{(x^2-\nu^2)^{1/2}+(y^2-\nu^2)^{1/2}}.$$

(7b)

The phase of the integrand is

$$\circledR = \left[(k_2 r')^2-\nu^2\right]^{1/2}+\left[(k_2 r)^2-\nu^2\right]^{1/2}-2(x^2-\nu^2)^{1/2}+2p(y^2-\nu^2)^{1/2}+$$

$$-\nu\cos^{-1}(\nu/k_2 r')-\nu\cos^{-1}(\nu/k_2 r)+2\nu\cos^{-1}(\nu/x)-2\nu p\cos^{-1}(\nu/y)+\nu\theta+2\pi m\nu,$$

(7c)

where the inverse cosine functions are bounded by 0 and π . If ν_σ is a point of stationary phase, the condition $\partial\circledR/\partial\nu\big|_{\nu_\sigma} = 0$ leads to

$$\cos^{-1}(\nu_\sigma/k_2 r') + \cos^{-1}(\nu_\sigma/k_2 r) - 2\cos^{-1}(\nu_\sigma/x) + 2p\cos^{-1}(\nu_\sigma/y) = \theta+2\pi m.$$

(8)

This equation does not have solutions for all values of m and p For a fixed value of p, for example, the left side of (8) has a maximum in (-A, A) which always occurs at $\nu_\sigma = -A$. As A approaches y this maximum

value approaches $2\pi p - U$, where

$$U = \cos^{-1}(y/k_2 r') + \cos^{-1}(y/k_2 r) - 2\cos^{-1} N .$$

On the other hand, at $\nu_\sigma = A$ the value is minimum and approaches U as

A approaches y. Since the right hand side of (8) must be within these limits,

the possible values of m satisfy

$$2\pi p - (U + \theta) > 2\pi m > U - \theta.$$

But m is an integer, and

$$\pi > U > 0, \qquad\qquad \pi \geq \theta \geq 0$$

so that

$$p - 1 \geq m \geq 1.$$

It is clear that for $m = 0$, (8) has a solution only when $\theta > U$. The

equation of the line separating regions 2 and 3 is $\theta = U$ (see figure 1).

The stationary phase evaluation of (7a) yields

$$I_{pm} \sim \left(\frac{2}{\pi}\right)^{\frac{1}{2}} \frac{(1+R_{1\sigma})(1+R_{2\sigma})(-R_{2\sigma})^{p-1} \exp\left\{i\left[\pi/4 + (p-1)\pi/2\right]\right\} \exp(i\Theta_\sigma)\left[1 + O(y^{-1})\right]}{\left\{\left[(k_2 r')^2 - \nu_\sigma^2\right]\left[(k_2 r)^2 - \nu_\sigma^2\right]\right\}^{\frac{1}{4}}\left\{\frac{2p}{(y^2 - \nu_\sigma^2)^{\frac{1}{2}}} - \frac{2}{(x^2 - \nu_\sigma^2)^{\frac{1}{2}}} + \frac{1}{\left[(k_2 r')^2 - \nu_\sigma^2\right]^{\frac{1}{2}}} + \frac{1}{\left[(k_2 r)^2 - \nu_\sigma^2\right]^{\frac{1}{2}}}\right\}^{\frac{1}{2}}} ,$$

$$(9a)$$

where the subscript σ denotes evaluation at ν_σ , and in particular

$$\Theta_\sigma = k_2\left\{\left[r'^2 - (\nu_\sigma/k_2)^2\right]^{\frac{1}{2}} + \left[r^2 - (\nu_\sigma/k_2)^2\right]^{\frac{1}{2}} - 2\left[a^2 - (\nu_\sigma/k_2)^2\right]^{\frac{1}{2}}\right\} +$$

$$+ 2p k_1\left[a^2 - (\nu_\sigma/k_1)^2\right]^{\frac{1}{2}} .$$

$$(9b)$$

The physical interpretation of these results as the rays of geometric optics is given in [1] . We note briefly that the function multiplying k_2 in (9b) is the distance the ray travels outside the cylinder, while the multiplicand of k_1 corresponds to the p equal paths the ray traverses inside. Thus the rays undergo $p-1$ internal reflections as is borne out by the factor $R_{2\sigma}^{p-1}$, since the quantities $R_{1\sigma}$, $R_{2\sigma}$, $(1 + R_{1\sigma})$, and $(1 + R_{2\sigma})$ are the Fresnel reflection and transmission coefficients. Furthermore when $m < p/2$ the ray encircles the origin m times in a counterclockwise direction, while for $m \geq p/2$, the clockwise encirclements are given by $p - m$. The localization principle [5] as well as Snell's law are verified by the interpretation of ν_σ/k as the distance from the ray to the origin, where $k = k_2$ for the external ray and k_1 for the internal. If α_i and α_r are respectively the angles of incidence and refraction we have

$$\sin \alpha_i = \nu_\sigma / k_2 \qquad\qquad \sin \alpha_r = \nu_\sigma / k_1$$

so that

$$\frac{\sin \alpha_i}{\sin \alpha_r} = \frac{k_1}{k_2} = N,$$

which is Snell's law. These quantities are illustrated in figure 2.

The integrals in (6a) and (6b) do not have stationary points in region 1; they are evaluated as residue sums. Only the lower half plane solutions of

$$x \frac{H_\nu^{(1)\prime}(x)}{H_\nu^{(1)}(x)} - y \frac{J_\nu^\prime(y)}{J_\nu(y)} = 0$$

(10)

are used to locate the poles of R (ν) since with $m < 0$ the integrals (6a) require that the contour be closed below the axis. The pole locations $\nu = -\nu_\ell$, as computed in [6] are shown in figure 3. The integrals in (6b) are similarly

evaluated at the poles of $R(-\nu)$ in the upper half plane, i.e. at $\nu = \nu_\ell$

Thus (6a) is equal to

$$\sum_{m=-\infty}^{-1} 2\pi i \sum_{\nu_\ell}^{-1} \frac{H_\nu^{(i)}(k_2 r') H_\nu^{(i)}(k_1 r)}{[H_\nu^{(i)}(x)]^2} \frac{x\left[H_\nu^{(i)}(x) H_\nu^{(2)'}(x) - H_\nu^{(2)}(x) H_\nu^{(i)'}(x)\right] e^{-i\nu\theta} e^{-2\pi i m\nu}}{\frac{\partial}{\partial \nu}\left\{x \frac{H_\nu^{(i)'}(x)}{H_\nu^{(i)}(x)} - y \frac{J_\nu'(y)}{J_\nu(y)}\right\}_{\nu=-\nu_\ell}} =$$

$$= i \sum_{m=-\infty}^{-1} \sum_{\nu_\ell} \frac{H_\nu^{(i)}(k_2 r') H_\nu^{(i)}(k_1 r)}{[H_\nu^{(i)}(x)]^2} \frac{e^{-i\nu\theta} e^{-2\pi i m\nu}}{\frac{\partial}{\partial \nu}\left\{x \frac{H_\nu^{(i)'}(x)}{H_\nu^{(i)}(x)} - y \frac{J_\nu'(y)}{J_\nu(y)}\right\}_{\nu=-\nu_\ell}} .$$

Under the conditions $\nu_\ell - x = O(x^{1/3})$ and $\nu_\ell - y = O(y)$, the asymptotic form of this residue sum is

$$\sum_{m=-\infty}^{-1} \sum_{\nu_\ell} \frac{1}{(2\pi)} \left(\frac{x}{2}\right)^{1/3} \frac{\exp\left\{ik_2\left[\sqrt{r'^2-(\nu/k_2)^2}+\sqrt{r^2-(\nu/k_1)^2}\right]-i\nu\left[\cos^{-1}\nu/k_2 r'+\cos^{-1}\nu/k_1 r+\theta+2\pi m\right]\right\}\left[1+O(x^{-1})\right]}{\left\{[(k_1 r')^2-\nu^2][(k_1 r)^2-\nu^2]\right\}^{1/4} \left[p(x,\nu) Ai(-q e^{-i\pi/3})\right]^2 \frac{\partial}{\partial \nu}\left\{x \frac{H_\nu^{(i)'}(x)}{H_\nu^{(i)}(x)} - y \frac{J_\nu'(y)}{J_\nu(y)}\right\}_{\nu=-\nu_\ell}} , \qquad (11a)$$

where

$$\frac{\partial}{\partial \nu}\left\{x \frac{H_\nu^{(i)'}(x)}{H_\nu^{(i)}(x)} - y \frac{J_\nu'(y)}{J_\nu(y)}\right\}_{-\nu_\ell} = -\frac{(\nu_\ell^2-y^2)}{x} + \frac{4(\nu_\ell^2-y^2)(\nu_\ell-x)}{15 x^2} + 2(\nu_\ell-x) + O(1), \qquad (11b)$$

$p(x,\nu)$ and q are the Schöbe polynomials [4], and Ai(η) is the Airy function of the first kind. Similarly (6b) becomes

$$\sum_{m=0}^{\infty} \sum_{\nu_\ell} \frac{1}{(2\pi)} \left(\frac{x}{2}\right)^{1/3} \frac{\exp\left\{ik_2\left[\sqrt{r'^2-(\nu/k_2)^2}+\sqrt{r^2-(\nu/k_1)^2}\right]-i\nu\left[\cos^{-1}\nu/k_2 r'+\cos^{-1}\nu/k_1 r-\theta-2\pi m\right]\right\}\left[1+O(x^{-1})\right]}{\left\{[(k_1 r')^2-\nu^2][(k_1 r)^2-\nu^2]\right\}^{1/4} \left[p(x,\nu) Ai(-q e^{i\pi/3})\right]^2 \frac{\partial}{\partial \nu}\left\{x \frac{H_\nu^{(i)'}(x)}{H_\nu^{(i)}(x)} - y \frac{J_{-\nu}'(y)}{J_{-\nu}(y)}\right\}_{\nu=\nu_\ell}} , \qquad (12)$$

where the derivative is given by (11b).

The terms (11a) and (12) represent the well-known creeping waves [1] ,
which radiate tangentially as they propagate around the cylinder. The exponential
decay depends on the product of the angle and $\text{Im}(\nu_\ell)$. Thus the only
important contributions are from the first encirclement, i.e. $m = 0$ and -1.
Physically, the waves have radiated away so much energy in their first encircle-
ment that their next contribution is negligible. The localization principle can
be applied to these waves also since $\nu_\ell \approx \chi$ for the counterclockwise waves
which are associated with rays striking the cylinder tangentially in $\theta > 0$;
for the clockwise waves, $-\nu_\ell \approx -\chi$, and the tangential rays are incident
in $\theta < 0$. The geometrical model is illustrated in figure 4.

For $\theta = \pi$, the terms in (11a) and (12) are identical since the geometry
is symmetrical about $\theta = 0$, π . Further, the residue sum for $m = 0$ does
not converge when

$$\cos^{-1}(\chi/k_2 r) + \cos^{-1}(\chi/k_2 r') = \theta,$$

which defines the common boundary of regions 1 and 2. Here the observation point
moves into the region of direct illumination, and the integral with $m = 0$ gives
optical rays.

Region 2

In region 2 it is convenient to rewrite the integral in (6b) with $m = 0$ as,

$$\frac{i}{8} \int_{-\infty}^{\infty} \left[H_\nu^{(1)}(k_2 r') H_\nu^{(2)}(k_2 r) + H_\nu^{(1)}(k_2 r') H_\nu^{(1)}(k_2 r) \frac{H_\nu^{(2)}(x)}{H_\nu^{(1)}(x)} R_1(\nu) \right] e^{i\nu\theta} d\nu + \tag{13a}$$

$$-\frac{1}{\pi^2} \int_{-\infty}^{\infty} \frac{H_\nu^{(1)}(k_2 r') H_\nu^{(1)}(k_2 r)}{[H_\nu^{(1)}(x)]^2 \, H_{-\nu}^{(2)}(y) \, J_{-\nu}(y)} \frac{e^{i\nu\theta}}{L(\nu)\left\{ x \frac{H_\nu^{(1)'}(x)}{H_\nu^{(1)}(x)} - y \frac{J_{-\nu}'(y)}{J_{-\nu}(y)} \right\}} d\nu. \tag{13b}$$

The first of these integrals (13a) is evaluated by the stationary phase technique. We obtain in part

$$\frac{i}{4}\left(\frac{2}{\pi}\right)^{\frac{1}{2}}\frac{exp\left[i\left(k_2|\vec{r}-\vec{r}'|-\pi/4\right)\right]}{\left(k_2|\vec{r}-\vec{r}'|\right)^{1/2}}\left\{1+O\left[\left(k_2r\right)^{-1}\right]\right\},$$

which is just the first term in the asymptotic series for $(i/4)\,H_0^{(1)}(k_2|\vec{r}-\vec{r}'|)$, the free space Green's function or equivalently the direct ray. In addition (13a) yields the singly reflected ray

$$\frac{R_{1\sigma}\;exp\left[i\left(\Theta_\sigma+\pi/4\right)\right]\left[1+O(x^{-1})\right]}{2\left(2\pi\right)^{1/2}\left\{\left[(k_2r')^2-\nu_\sigma^2\right]\left[(k_2r)^2-\nu_\sigma^2\right]\right\}^{1/4}\left\{\frac{2}{(x^2-\nu_\sigma^2)^{1/2}}-\frac{1}{\left[(k_2r')^2-\nu_\sigma^2\right]^{1/2}}-\frac{1}{\left[(k_2r)^2-\nu_\sigma^2\right]^{1/2}}\right\}^{1/2}},$$

where

$$\Theta_\sigma=k_2\left\{\left[r'^2-(\nu_\sigma/k_2)^2\right]^{1/2}+\left[r^2-(\nu_\sigma/k_2)^2\right]^{1/2}-2\left[a^2-(\nu_\sigma/k_2)^2\right]^{1/2}\right\},$$

$$R_{1\sigma}=\begin{cases}\dfrac{(x^2-\nu_\sigma^2)^{1/2}-(y^2-\nu_\sigma^2)^{1/2}}{(x^2-\nu_\sigma^2)^{1/2}+(y^2-\nu_\sigma^2)^{1/2}}&\nu_\sigma<y\\[1em]\dfrac{(x^2-\nu_\sigma^2)^{1/2}+i(\nu_\sigma^2-y^2)^{1/2}}{(x^2-\nu_\sigma^2)^{1/2}-i(\nu_\sigma^2-y^2)^{1/2}}&\nu_\sigma>y,\end{cases}$$

and ν_σ is the solution of

$$\cos^{-1}(\nu_\sigma/k_2r')+\cos^{-1}(\nu_\sigma/k_2r)-2\cos^{-1}(\nu_\sigma/x)=\Theta.$$

Here we have neglected the phase contributed by $R_1(\nu)$ for $\nu>y$ since it is of a lower order than that given by the Hankel functions.

The integral (13b) is evaluated as a residue sum at the poles of the integrand in the upper half plane. These are the solutions of $L(\nu)=0$,

$$x\,\frac{H_\nu^{(1)'}(x)}{H_\nu^{(1)}(x)}-y\,\frac{H_\nu^{(2)'}(y)}{H_\nu^{(2)}(y)}=0$$

$$(14a)$$

as well as the solutions of

$$x \frac{H_\nu^{(1)\prime}(x)}{H_\nu^{(1)}(x)} - y \frac{J_{-\nu}^{\prime}(y)}{J_{-\nu}(y)} = 0.$$

(14b)

The solutions of (14b) in the upper half plane are ν_ℓ , while those of (14a) are ν_ℓ and ν_s (see figure 5). Thus it appears that double poles exist at ν_ℓ ; however, an examination of equations (14a) and (14b) shows that these solutions are not exactly coincident and in fact depend on $2 J_{-\nu}(y) \sim H_{-\nu}^{(2)}(y)$ in this part of the ν plane. By writing $\nu_\ell^{\prime}$ for the roots of (14a) and $\nu_\ell^{\prime\prime}$ for those of (14b) we show in Appendix B that the total residue contribution at ν_ℓ is negligible.

Thus (13b) is equal to

$$\sum_{\nu_s} i \cdot \frac{H_{\nu_s}^{(1)}(k_2 r') \, H_{\nu_s}^{(1)}(k_1 r)}{\left[H_{\nu_s}^{(1)}(x) \right]^2} \cdot \frac{e^{i\nu_s \theta}}{\dfrac{\partial}{\partial \nu}\left\{ x \dfrac{H_\nu^{(1)\prime}(x)}{H_\nu^{(1)}(x)} - y \dfrac{H_\nu^{(2)\prime}(y)}{H_\nu^{(2)}(y)} \right\}_{\nu_s}}$$

which becomes after substitution of the asymptotic forms

$$\sum_{\nu_s} i \left\{ \frac{(x^2 - \nu_s^2)^2}{[(k_2 r')^2 - \nu_s^2][(k_1 r)^2 - \nu_s^2]} \right\}^{1/4} \frac{[1 + O(x^{-1})]}{\dfrac{\partial}{\partial \nu}\left\{ x \dfrac{H_\nu^{(1)\prime}(x)}{H_\nu^{(1)}(x)} - y \dfrac{H_\nu^{(2)\prime}(y)}{H_\nu^{(2)}(y)} \right\}_{\nu_s}} \exp\left\{ i k_2 \left[\sqrt{r'^2 - (\nu_s/k_2)^2} \right. \right.$$

$$\left. + \sqrt{r^2 - (\nu_s/k_2)^2} - 2\sqrt{a^2 - (\nu_s/k_a)^2} \right] - i\nu_s \left[\cos^{-1}(\nu_s/k_1 r') + \cos^{-1}(\nu_s/k_1 r) + \right.$$

$$\left. \left. - 2\cos^{-1}(\nu_s/x) - \theta \right] \right\}$$

(15a)

where

$$\frac{\partial}{\partial \nu}\left\{ x \frac{H_\nu^{(1)\prime}(x)}{H_\nu^{(1)}(x)} - y \frac{H_\nu^{(2)\prime}(y)}{H_\nu^{(2)}(y)} \right\}_{\nu_s} \sim -\frac{(x^2 - \nu_s^2)}{y} + \frac{4(x^2 - \nu_s^2)(\nu_s - y)}{15 y^2} + 2(\nu_s - y) + O(1) = O(x).$$

(15b)

It is possible to interpret formulae (15a) and (15b) in terms of ray

optics, but not as clearly as in the creeping wave situation. Since $\nu_s \approx -y + i\,Im(\nu_s)$

where $Im(\nu_s) > 0$, the localization principle relates these terms to the rays

which strike the cylinder at the angle of total reflection above the line $\theta = 0$.

The first phase term in (15a) is the product of k_2 and a distance consistent with

the above interpretation (see figure 6). The second phase term

$$- i\nu_s \left[\cos^{-1}(\nu_s/k_2 r') + \cos^{-1}(\nu_s/k_2 r) - 2\cos^{-1}(\nu_s/x) - \theta \right]$$

is approximately equal to

$$i\nu_s \left[\theta + \cos^{-1}(Na/r') + \cos^{-1}(Na/r) - 2\cos^{-1}N \right],$$

which is $i\nu_s$ multiplying the angle Ω shown in figure 6. Thus this part of the

phase represents a wave traveling counterclockwise around the cylinder with

propagation constant ν_s . Since $Im(\nu_s) > 0$, the exponential in (15a) has

a negative real part and the wave decays in proportion to the angle; however,

the $Re(\nu_s)$ is negative and so the physical interpretation is not completely

satisfactory.

Region 3

The results derived above for (13a) and (13b) are applicable to

observation points in region 3. The integrals (5c), however, as was mentioned in

connection with equation (8), have no stationary phase points in region 3. After

summation (5c) is equal to

$$- \frac{i}{\pi^2} \int_{-\infty}^{\infty} \frac{H_\nu^{(1)}(k_2 r') \, H_\nu^{(1)}(k_2 r)}{[H_\nu^{(1)}(x)]^2 \, H_\nu^{(2)}(y) \, J_\nu(y) \, L(\nu)} \frac{e^{i\nu\theta}}{\left\{ x \frac{H_\nu^{(1)\prime}(x)}{H_\nu^{(1)}(x)} - y \frac{J_\nu'(y)}{J_\nu(y)} \right\}} \, d\nu \, , \tag{16}$$

which is evaluated by residues.

For $\theta > 0$, the contour may only be closed by an infinite semicircle

in the upper half plane. The four residue series obtained from the poles $\nu_p, \nu_s, \nu_q,$

and $\vec{V}_\lambda$ (see figures 3 and 5) converge so slowly that one could as well employ the series solution (2α). It is, however, possible to approximate (16) by deforming the path of integration as shown in figure 7. The integral over the new path is neglected compared to the residues at the captured poles, $-\vec{V}_s$, (see Appendix C). We note that the residues at the captured poles, $-\vec{V}_\ell$, are negligible as shown in Appendix B. Thus (16) is approximately equal to

$$\sum_{\vec{V}_s}' i \left\{ \frac{(x^2 - \vec{V}_s^2)^2}{[(k_1 r)^2 - \vec{V}_s^2][(k_2 r)^2 - \vec{V}_s^2]} \right\}^{1/4} \frac{[1 + O(x^{-1})]}{\frac{\partial}{\partial \nu} \left\{ x \frac{H_\nu^{(1)'}(x)}{H_\nu^{(1)}(x)} - y \frac{H_\nu^{(1)'}(y)}{H_\nu^{(1)}(y)} \right\}_{\vec{V}_s}} \cdot$$

$$\cdot \exp \left\{ i k_2 \left[\sqrt{r'^2 - (\vec{V}_s/k_2)^2} + \sqrt{r^2 - (\vec{V}_s/k_2)^2} - 2\sqrt{a^2 - (\vec{V}_s/k_2)^2} \right] + \right.$$

$$\left. - i\vec{V}_s \left[\cos^{-1}(\vec{V}_s/k_2 r') + \cos^{-1}(\vec{V}_s/k_2 r) - 2\cos^{-1}(\vec{V}_s/x) + \theta \right] \right\}$$

$$(17)$$

where the summation includes only captured poles and the derivative is given by (15b). In region 3 the inequality

$$\cos^{-1}(Na/r') + \cos^{-1}(Na/r) - 2\cos^{-1}(N) > \theta \tag{18}$$

is satisfied and successive terms in (17) have decreasing magnitudes.

The form of (17) is the same as (15a) with the sign of θ reversed; indeed for $\theta = 0$ the integrals (16) and (13b) are identical. The physical interpretation of the residues at $\vec{V}_s$ and $-\vec{V}_s$ is similar except that the former are associated with rays incident in $\theta > 0$.

Plane Waves and Back-Scattering

To specialize the above results to the case of an incident plane wave of unit amplitude, one simply applies the operator

$$\lim_{r' \to \infty} -4i (\pi k_2 r'/2)^{1/2} \exp \left[i (\pi/4 - k_2 r') \right]$$

to the previous results. We choose here to consider the case of back-scattering

since the other case of chief interest, the scattering cross section, cannot be completely treated by the methods developed above.

The normalized back-scattering cross section is defined by

$$\sigma_B = \left| \lim_{r \to \infty} \left(\frac{2r}{a} \right)^{\frac{1}{2}} E_S (\theta = 0) \right|^2 = |E_R|^2$$

where E_B is the scattered field, and

$$E_R =$$

$$= \left(\frac{1-N}{1+N} \right) e^{-2ix} + \sum_{p=2}^{\infty} \sum_{m=1}^{p-1} (1 + R_{1\sigma})(1 + R_{2\sigma})(-R_{2\sigma})^{p-1} \left\{ \frac{\cos \alpha_i}{\frac{p \cos \alpha_i}{N \cos \alpha_r} - 1} \right\}^{1/2} \cdot$$

$$\cdot \exp \left\{ -2ix \left(1 - pN \frac{\cos \alpha_r}{\cos \alpha_i} \right) + i \frac{\pi}{2} (p-1) \right\} +$$

(19a)

$$+ 2 \left(\frac{2}{x} \right)^{1/3} \sum_{m=1}^{\infty} \sideset{}{'}\sum_{\nu_\ell} \frac{x \exp \left[i \nu_\ell (2m-1) \pi + i \pi/4 \right]}{(\nu_\ell^2 - y^2) \left\{ p(x, \nu_\ell) A_i \left[-q(x, \nu_\ell) e^{-i\pi/3} \right] \right\}^2} +$$

(19b)

$$- 8 \left(\frac{\pi}{2} \right)^{\frac{1}{2}} \sideset{}{'}\sum_{\nu_s} \frac{y}{(x^2 - \nu_s^2)^{1/2}} \exp \left\{ -2ix \left(1 - \nu_s^2/x^2 \right)^{1/2} - i \nu_s \left(\pi - 2 \cos^{-1} \nu_s/x \right) - i \pi/4 \right\}$$

(19c)

with $\cos \alpha_i = \left(1 - \nu_\sigma^2/x^2 \right)^{\frac{1}{2}}$ and $\cos \alpha_r = \left(1 - \nu_\sigma^2/y^2 \right)^{\frac{1}{2}}$.

The calculation of σ_B was programmed for the IBM 7070 of the Brown University Computing Center. The geometric optics terms in (19a) required the iterative solution of

$$\sin \alpha_i = N \sin \alpha_r$$

and

$$\alpha_r = \frac{1}{p} \left[\alpha_i - \pi (p/2 - m) \right].$$

The creeping wave terms represented by (19b) were found to be negligible and only (19c) contributed to the diffraction effect. Figure 8 is a plot of σ_g vs $k_2 a$ for N = .4.

The results developed here do not apply to observation points near $\theta = \pi$ and the boundaries separating regions 1, 2 and 3 since these lines are caustics. Thus the forward scatter with an incident plane wave has not been completely determined and the scattering cross section cannot be calculated.

Appendix A

The power series (4a)

$$R(\nu) = R_1(\nu) + (1+R_1)(1+R_2)\sum_{p=1}^{\infty} R_2^{p-1}\left[H_\nu^{(1)}(y)/H_\nu^{(2)}(y)\right]^p$$

converges by the ratio test when

$$\left| R_2\, H_\nu^{(2)}(y)/H_\nu^{(1)}(y)\right| < 1.$$

On the real ν axis this condition becomes $|R_2| < 1$ or $R_2 R_2^* < 1$.

We write

$$R_2 = -\frac{D-NE}{D-NE^*}$$

so that

$$R_2 R_2^* = \frac{|D|^2 + N^2 |E|^2 - N(ED^* + DE^*)}{|D|^2 + N^2 |E|^2 - N(E^* D^* + DE)}.$$

(A-1)

We have, however,

$$ED^* + DE^* - (E^* D^* + DE) = -(D - D^*)(E - E^*)$$

(A-2)

where

$$D - D^* = \frac{H_\nu^{(1)'}(x)}{H_\nu^{(1)}(x)} - \frac{H_\nu^{(2)'}(x)}{H_\nu^{(2)}(x)} = \frac{4i}{\pi x \, |H_\nu^{(1)}(x)|^2}$$

and

$$E - E^* = \frac{4i}{\pi y \, |H_\nu^{(1)}(y)|^2},$$

so that (A-2) is positive definite. This implies that (A-1) is less than unity and the series converges.

Appendix B

At the solutions of (14a), ν_ℓ' , the residue calculation gives for the denominator of (13b)

$$H_{-\nu}^{(2)}(y) \, J_{-\nu}(y) \left\{ x \frac{H_\nu^{(1)'}(x)}{H_\nu^{(1)}(x)} - y \frac{J_{-\nu}'(y)}{J_{-\nu}(y)} \right\} \frac{\partial}{\partial \nu} \left\{ x \frac{H_\nu^{(1)'}(x)}{H_\nu^{(1)}(x)} - y \frac{H_\nu^{(2)'}(y)}{H_\nu^{(2)}(y)} \right\}_{\nu_\ell'} =$$

$$= y \left[H_{-\nu}^{(2)'}(y) \, J_{-\nu}(y) - H_{-\nu}^{(2)}(y) \, J_{-\nu}'(y) \right] \frac{\partial}{\partial \nu} \left\{ x \frac{H_\nu^{(1)'}(x)}{H_\nu^{(1)}(x)} - y \frac{H_\nu^{(2)'}(y)}{H_\nu^{(2)}(y)} \right\}_{\nu_\ell'} =$$

$$= - \frac{2i}{\pi} \, \frac{\partial}{\partial \nu} \left\{ x \frac{H_\nu^{(1)'}(x)}{H_\nu^{(1)}(x)} - y \frac{H_\nu^{(2)'}(y)}{H_\nu^{(2)}(y)} \right\}_{\nu_\ell'} \, ,$$

where the Wronskian relation has been employed. Similarly at the solutions of (14b), ν_ℓ'' , we have

$$H_{-\nu}^{(1)}(y) \, J_{-\nu}(y) \left\{ x \frac{H_\nu^{(1)'}(x)}{H_\nu^{(1)}(x)} - y \frac{H_\nu^{(2)'}(y)}{H_\nu^{(2)}(y)} \right\} \frac{\partial}{\partial \nu} \left\{ x \frac{H_\nu^{(1)'}(x)}{H_\nu^{(1)}(x)} - y \frac{J_{-\nu}'(y)}{J_{-\nu}(y)} \right\}_{\nu_\ell''} =$$

$$= \frac{2i}{\pi} \, \frac{\partial}{\partial \nu} \left\{ x \frac{H_\nu^{(1)'}(x)}{H_\nu^{(1)}(x)} - y \frac{J_{-\nu}'(y)}{J_{-\nu}(y)} \right\}_{\nu_\ell''} \, .$$

Adding the two residues and setting $\nu_\ell' = \nu_\ell'' = \nu_\ell$, the result is

$$\frac{\pi}{2i} \frac{y \frac{\partial}{\partial \nu} \left\{ \frac{H_\nu^{(2)'}(y)}{H_\nu^{(2)}(y)} - \frac{J_{-\nu}'(y)}{J_{-\nu}(y)} \right\}}{\frac{\partial}{\partial \nu} \left\{ x \frac{H_\nu^{(1)'}(x)}{H_\nu^{(1)}(x)} - y \frac{H_\nu^{(2)'}(y)}{H_\nu^{(2)}(y)} \right\} \frac{\partial}{\partial \nu} \left\{ x \frac{H_\nu^{(1)'}(x)}{H_\nu^{(1)}(x)} - y \frac{J_{-\nu}'(y)}{J_{-\nu}(y)} \right\}} \Bigg|_{\nu_\ell} \sim$$

$$\sim - \frac{\frac{\partial}{\partial \nu} \left\{ \frac{e^{2\pi i \nu}}{[H_\nu^{(2)}(y)]^2} \right\}}{\left\{ \frac{\partial}{\partial \nu} \left[x \frac{H_\nu^{(1)'}(x)}{H_\nu^{(1)}(x)} - y \frac{H_\nu^{(2)'}(y)}{H_\nu^{(2)}(y)} \right] \right\}^2} \Bigg|_{\nu_\ell} \sim \frac{2 x^2 \cosh^{-1}(\nu_\ell/y) \exp(2\pi i \nu_\ell)}{(\nu_\ell^2 - y^2) \left[H_{\nu_\ell}^{(2)}(y) \right]^2}$$

which is very small since $Im(\nu_\ell) > 0$ and $H_{\nu_\ell}^{(2)}(y)$ increases as an exponential function of ν_ℓ .

The residues of (16) at $-\nu_\ell$ yield the same result, as substitution of $-\nu$ for ν will show.

Appendix C

On those parts of the path shown in figure 7, which coincide with the real axis, the integrand of (16)

$$\frac{H_\nu^{(1)}(k_2 r') \, H_\nu^{(1)}(k_2 r) \; e^{i\nu\theta}}{[H_\nu^{(1)}(x)]^2 \, H_\nu^{(2)}(y) \, J_\nu(y) \, L(\nu) \left\{ x \dfrac{H_\nu^{(1)\prime}(x)}{H_\nu^{(1)}(x)} - y \dfrac{J_\nu'(y)}{J_\nu(y)} \right\}} \tag{C-1}$$

has an exponential variation given by

$$\frac{H_\nu^{(1)}(k_2 r') \, H_\nu^{(1)}(k_2 r)}{[H_\nu^{(1)}(x)]^2} \; e^{i\nu\theta} \quad . \tag{C-2}$$

When $|\nu| > x$ and $|\nu| - x \sim O(x)$, (C-2) is very small and decreases rapidly with increasing $|\nu|$.

The exponential variation of (C-1) on the circular part of the path changes from (C-2) on the arc PQ to

$$\frac{H_\nu^{(1)}(k_2 r') \, H_\nu^{(1)}(k_2 r)}{[H_\nu^{(1)}(x)]^2 \, [H_\nu^{(2)}(y)]^2} \; e^{i\nu\theta} \tag{C-3}$$

on the arc QRS (see figure 7). Since (C-2) is symmetric about the imaginary axis and $[H_\nu^{(2)}(y)]^{-2}$ is very small in the third quadrant, the maximum value of (C-1) occurs on the arc PQR. Along PQR, (C-2) increases from

$$\exp\left[+2(\nu^2 - x^2)^{1/2} - 2\nu \cosh^{-1}(\nu/x) \right]$$

at P, to exp ($i\nu\theta$) at R. However, (C-3) must be employed at points between Q and R, and the additional quantity $\left[H_\nu^{(2)}(y) \right]^{-2}$ varies exponentially from unity at Q to exp ($-i\nu\pi$) at R. Thus the integrand (C-1) attains its maximum value in the vicinity of Q.

At Q the exponential variation of (C-1) is

$$\exp i\left\{ \left[(k_2r')^2 - \nu^2 \right]^{1/2} + \left[(k_2r)^2 - \nu^2 \right]^{1/2} - 2\left[x^2 - \nu^2 \right]^{1/2} - \nu \left[\cos^{-1}(\nu/k_2r') + \right.\right.$$

$$\left.\left. + \cos^{-1}(\nu/k_2r) - 2\cos^{-1}(\nu/x) + \theta \right] \right\},$$

(C-4)

and the equation of the curve passing through Q is

$$\text{Im}\left[(y^2 - \nu^2)^{1/2} - \nu \cos^{-1}(\nu/y) \right] = 0.$$

(C-5)

Since a general examination of (C-4) subject to (C-5) is quite complicated, a numerical example will be considered. Let k_2r', $k_2r = 3.5x$, $N = y/x = .5$, and $|\nu| = 1.4x$. An approximate solution of (C-5) yields $\nu = 1.4x \exp(-i\pi/4)$ and (C-4) is approximately equal to $\exp\left[x(-1.27 + \theta) \right]$. From (18), which defines region 3, we obtain $\theta < .76$ radians and the integral over the semicircle is negligible compared to the residues.

References

1. P. Beckmann and W. Franz, Z. Naturf. 12a, 257 (195).

2. P. Beckmann and W. Franz, IRE AP-4, 3 (1956).

3. T. T. Wu, Phys. Rev. 104, 1201 (1956).

4. W. Streifer and R. D. Kodis, Brown University Scientific Report AF 4561/17, June 1962.

5. H. C. van de Hulst, Light Scattering by Small Particles, (John Wiley, 1957).

6. W. Streifer and R. D. Kodis, Brown University Scientific Report (1962).
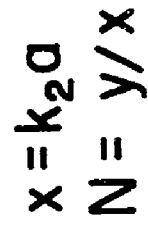
FIG. 1   REGIONS FOR OBSERVATION POINTS

$$\left[r'^2 - (\nu_\sigma/k_2)^2 \right]^{1/2} - \left[a^2 - (\nu_\sigma/k_2)^2 \right]^{1/2}$$

$(1+R_{1\sigma})$

a

$R_{1\sigma}$

α_i

α_i

α_r

ν_σ/k_2

ν_σ/k_1

$R_{2\sigma}(1+R_{1\sigma})$

θ

$\bar{r}^i$

$\bar{r}$

Unit incident ray

Snell's law:

$$\frac{\sin \alpha_i}{\sin \alpha_r} = N = \frac{k_1}{k_2} = \frac{\nu_\sigma/k_2}{\nu_\sigma/k_1}$$
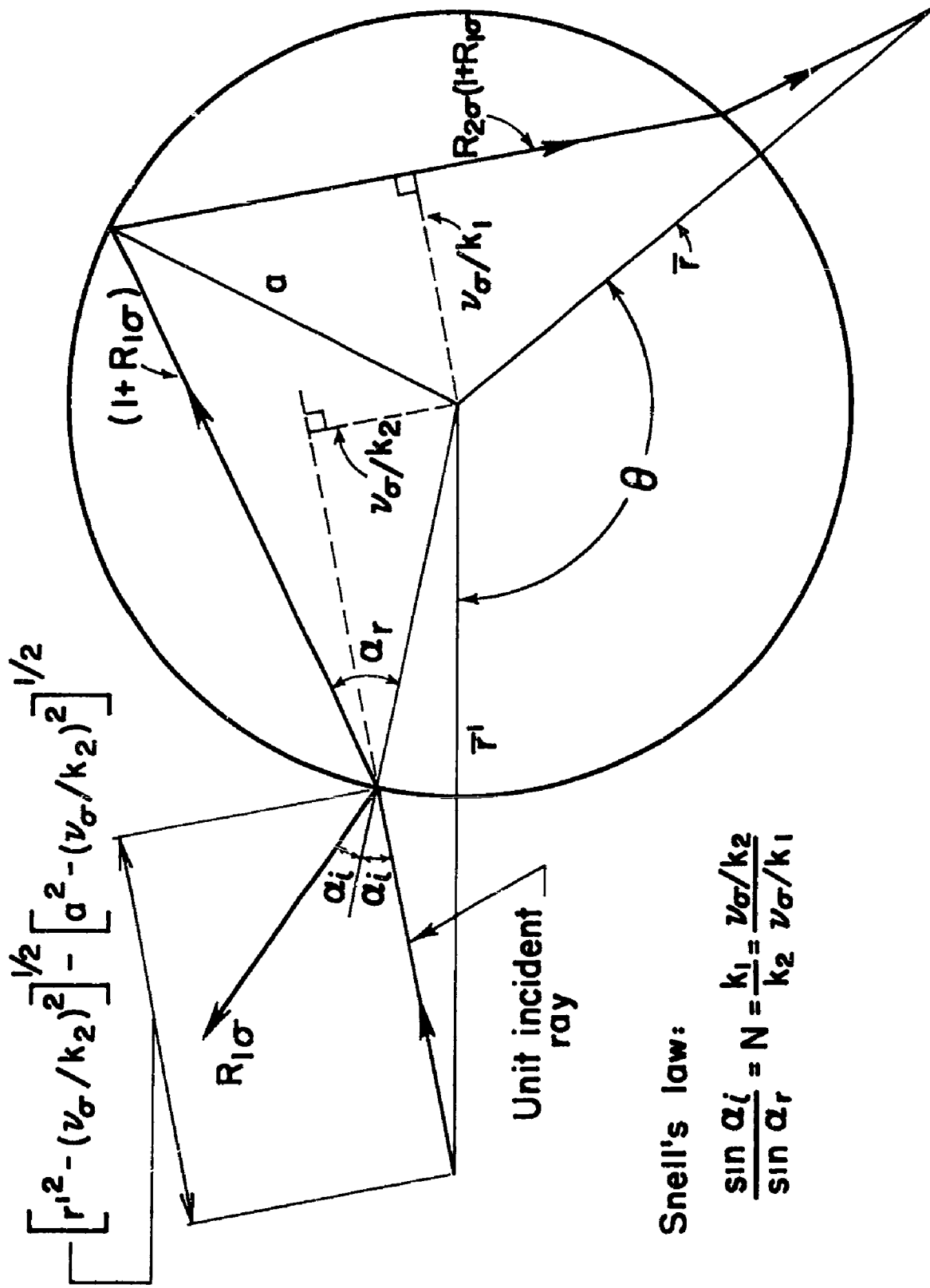
FIG. 2   A REFRACTED RAY, p=2, m=1
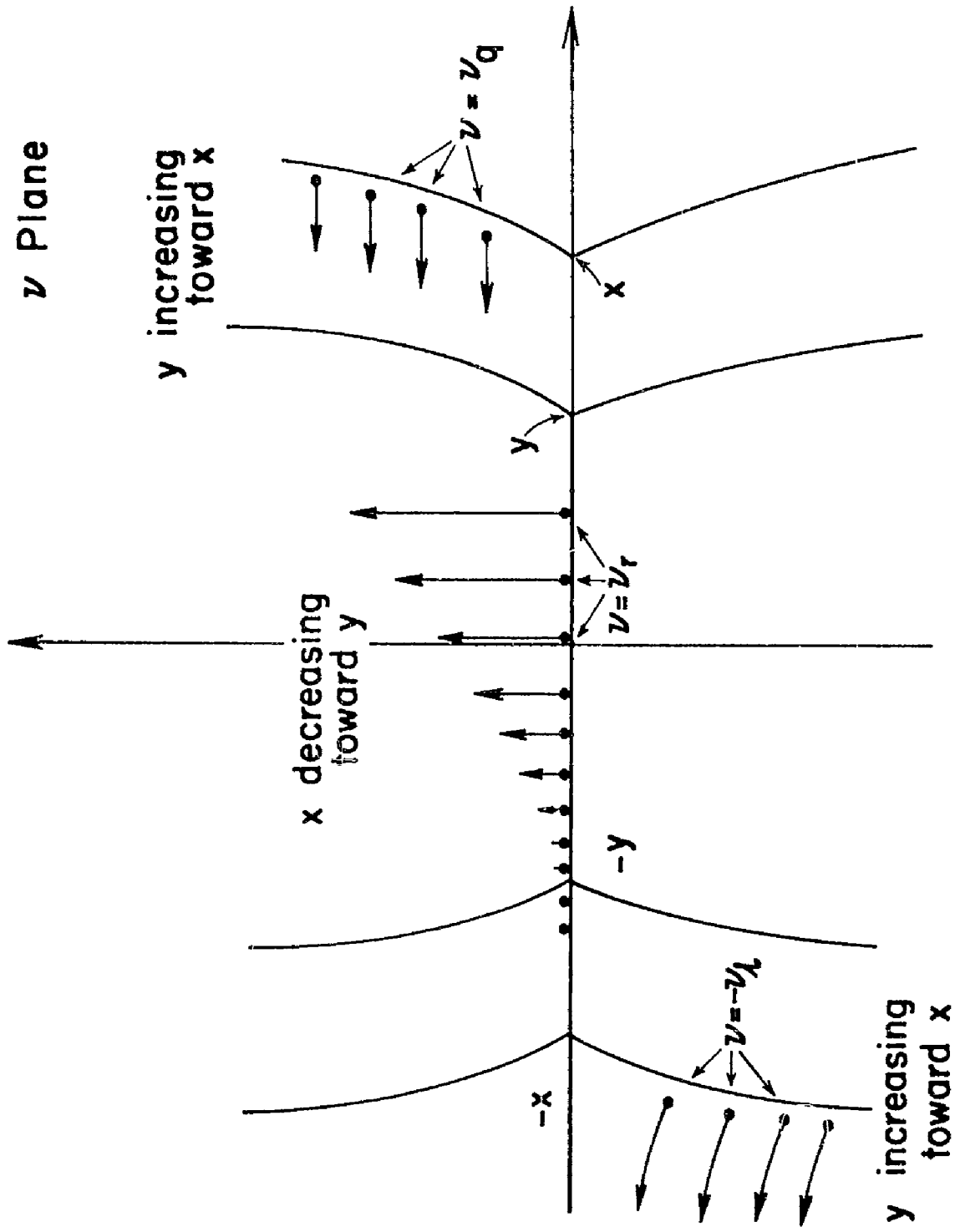
FIG. 3 ROOTS OF $x \dfrac{H_\nu^{(1)'}(x)}{H_\nu^{(1)}(x)} - y \dfrac{J_\nu'(y)}{J_\nu(y)} = 0$

$\cos^{-1}a/r^{-1}$

$\cos^{-1}a/r$

r^1

r

θ

a

$\sqrt{r'^2-a^2}$

$\sqrt{r^2-a^2}$

$a(\theta-\cos^{-1}a/r^1-\cos^{-1}a/r)$

(a)

$a(2\pi-\cos^{-1}a/r^1-\cos^{-1}a/r-\theta)$

$\sqrt{r'^2-a^2}$

a

$\sqrt{r^2-a^2}$

$\cos^{-1}a/r^1$

$\cos^{-1}a/r$

r^1

θ

r

(b)

FIG. 4 CREEPING WAVES
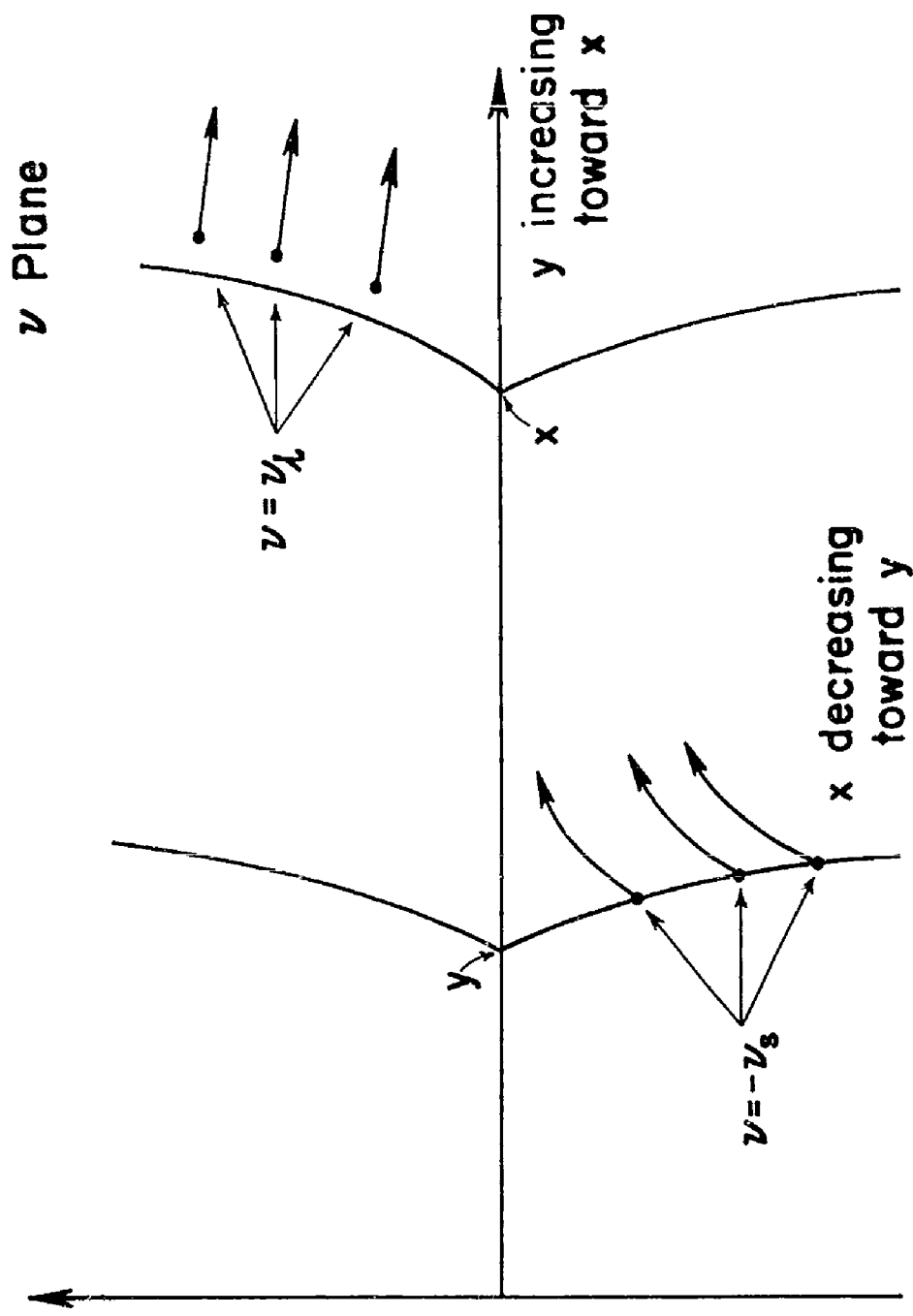
FIG.5 ROOTS OF $x \dfrac{H_\nu^{(1)'}(x)}{H_\nu^{(1)}(y)} - y \dfrac{H_\nu^{(2)'}(y)}{H_\nu^{(2)}(y)} = 0$

IN THE RIGHT HALF PLANE

FIG.6 PHYSICAL INTERPRETATION OF RESIDUES, EQUATION(15a)
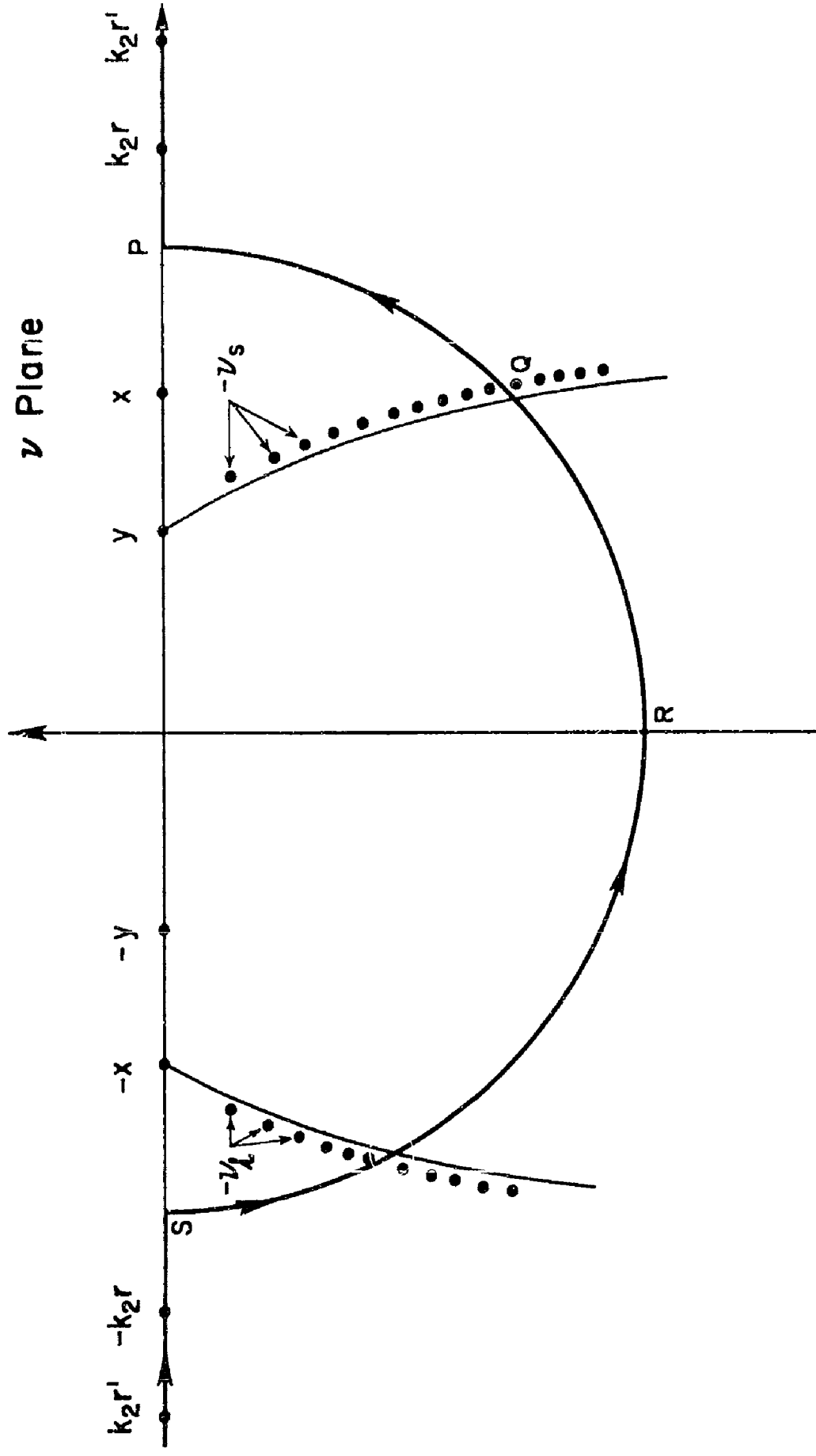
FIG. 7 DEFORMED PATH OF INTEGRATION

FIG. 8   NORMALIZED BACK-SCATTERING CROSS SECTION vs X

UNCLASSIFIED